Plant Physiology and Biochemistry 232 (2026) 111091

Contents lists available at ScienceDirect

Plant Physiology and Biochemistry

journal homepage: www.elsevier.com/locate/plaphy

Deciphering the unique selenocystathionine metabolism of the hyperaccumulator *Neptunia amplexicaulis*

Maggie-Anne Harvey [a,b], Antony van der Ent [a,b,*], Jason K. Kirby [c], Jemma I. Virtue [e], Clinton J. Kidman [d], James H. Lovett [e], Peter D. Erskine [b], Hugh H. Harris [e]

[a] Laboratory of Genetics, Wageningen University and Research, the Netherlands
[b] Centre for Mined Land Rehabilitation, Sustainable Minerals Institute, The University of Queensland, Queensland, Australia
[c] CSIRO Land and Water, Industry Environments Program, Adelaide, South Australia, Australia
[d] Department of Geological Sciences, University of Saskatchewan, Saskatoon, SK S7N 5E2, Canada
[e] Department of Chemistry, The University of Adelaide, Australia

ARTICLE INFO

Keywords:
hyperaccumulator
Methylselenocysteine
Selenium
Selenocystathionine
Neptunia amplexicaulis
Neptunia heliophila

ABSTRACT

- The legume *Neptunia amplexicaulis*, endemic to a small area in Central Queensland (Australia), is one of the strongest selenium hyperaccumulator plants known on Earth. This research aimed to examine the chemical speciation of selenium in this species to gain better understanding of the mechanism(s) of selenium tolerance in plant species for potential biofortification, bioremediation and pharmaceutical applications.
- *Neptunia amplexicaulis* and the comparative non-accumulator *Neptunia heliophila* were exposed to selenate (SeO_4^{2-}) and selenite (SeO_3^{2-}) and analysed using a combination of synchrotron-based X-ray fluorescence techniques and High-Performance Liquid Chromatography with Inductively Coupled Plasma – Mass Spectrometry (ICP-MS) and Liquid Chromatography - Tandem Mass Spectrometry (LC-MS).
- The study findings shows that selenocystathionine is the dominant chemical species of selenium in *N. amplexicaulis*. Minor amounts of selenate were found in the stems, while elemental selenium was identified in the roots.
- The accumulation of selenium in *N. amplexicaulis* organs differs from other selenium hyper-accumulators from the USA, in which methylselenocysteine dominates. Inorganic and elemental selenium play a fundamental role in hyperaccumulation, and their chemical analysis is highly challenging, but a combination of *in situ* and hyphenated techniques has proven to be powerful to unequivocally determine prevailing selenium chemical species in plant organs.

1. Introduction

Selenium (Se) is considered an essential element for nutrition in humans and animals but can become toxic at higher concentrations (Schwarz and Foltz, 1957; Rotruck et al., 1973; Rayman, 2008). For animals and some algal protists, Se is considered essential as it is a component in seleno-proteins, but the genetic capacity for seleno-protein production in most plants and some invertebrates seems to have been lost independently over time (Lobanov et al., 2007). To date, Se accumulation in plants has been shown to be beneficial but not essential for growth, development, or reproduction (White et al., 2004; Hartikainen, 2005; Pilon-Smits et al., 2009). Some plants have adapted to accumulate very high concentrations of Se in their organs, particularly for those found growing on Se-enriched soils (Rosenfeld and Beath, 1964; White, 2016; Schiavon and Pilon-Smits, 2017a). These 'Se hyperaccumulators' can accumulate over 1000 μg Se g^{-1}, while other

* Corresponding author. Laboratory of Genetics, Wageningen University and Research, the Netherlands.
E-mail address: antony.vanderent@wur.nl (A. van der Ent).

https://doi.org/10.1016/j.plaphy.2026.111091
Received 21 November 2025; Received in revised form 27 January 2026; Accepted 28 January 2026
Available online 31 January 2026

plants growing on seleniferous soils can be secondary Se accumulators (100–1000 μg Se g^{-1}) or non-accumulators (<100 μg Se g^{-1}) that tend towards exclusion of Se from their tissues (Brown and Shrift, 1982; Anderson, 1993). Selenium hyperaccumulators can be distinguished by higher leaf selenium to sulphur ratios, a high expression of root sulphate transporters and developed metabolic mechanisms to prevent the incorporation of Se into proteins (White, 2016). Some notable Se hyperaccumulators include species within the *Astragalus* genus (Fabaceae; particularly *A. bisulcatus* and *A. racemosus*), *Stanleya pinnata* and *Cardamine enshiensis* (Brassicaceae) and *Neptunia amplexicaulis* (Fabaceae) (Beath et al., 1939; Yuan et al., 2013; Schiavon and Pilon-Smits, 2017a).

1.1. Selenium speciation in hyperaccumulator plant species

The biochemistry of Se is complex, and the biological actions of Se are not properties of the element, but of its various chemical forms. Selenium hyperaccumulation in plants is likely a result of inorganic Se uptake through the root system via sulphate pathways for the bioavailable compound selenate (SeO_4^{2-}), and upregulation of the SULTR-1; 2 and SULTR-2; 1 genes responsible for the root sulphate transporters and efficient root to shoot translocation (Anderson, 1993; Hopper and Parker, 1999). Conversely selenite (SeO_3^{2-}), which becomes more bioavailable in waterlogged soils, is transported into plants through phosphate pathways (Shrift and Ulrich, 1969; Mikkelsen et al., 1989; Fordyce, 2013). Most metabolism of Se is thought to occur in the plastids of cells through the sulphate assimilation pathway – inorganic selenate in the cell enters the plastid to be reduced to adenosine phosphoselenate, then selenite, then selenide - or selenite entering the plastid is gradually reduced to selenide - then incorporated into the amino acid selenocysteine (SeCys) (Leustek and Saito, 1999; Sors et al., 2005; Cao et al., 2013). SeCys can be adventitiously incorporated into proteins in the place of cysteine (Cys) or follow the pathway for the formation of the amino acid selenomethionine (SeMet) through the formation of selenocystathionine (SeCT) as an intermediate (Terry et al., 2000; Van Huysen et al., 2003; Sors et al., 2005). SeCys can also form methylselenocysteine (MeSeCys) through the action of the selenocysteine methyltransferase (SMT) enzyme (Neuhierl and Böck, 1996). From there, MeSeCys could form γ-glutamyl-methyl selenocysteine (γ-GluMeSeCys) or be volatilised and released as the gas dimethyldiselenide (DMDSe) (Pilon-Smits and LeDuc, 2009). Conversely, SeCys may be cleaved to form elemental Se and alanine via the selenocysteine lyase activity of CpNifS (Pilon-Smits et al., 2002; Schiavon and Pilon-Smits, 2017a)

Selenium in hyperaccumulators is primarily metabolised into MeSeCys or γ-GluMeSeCys via constitutively expressed SMT in *Astragalus spp.* and *S. pinnata,* or SeCT, which tends to occur in smaller concentrations (Anderson, 1993; Pilon-Smits et al., 1999; Pickering et al., 2003; Freeman et al., 2006; Van Hoewyk et al., 2008). These amino acids are not commonly incorporated into proteins, unlike SeCys and SeMet, which can be over-incorporated in the place of their S-based counterparts, Cys and Met, and play a part in Se toxicity in plants (Stadtman, 1990; Van Hoewyk, 2013). In non-accumulator plants the Se tends to be present as inorganic Se species (*e.g.*, selenate) or as SeMet (Tagmount et al., 2002; Pickering et al., 2003; Lima et al., 2018).

1.2. Neptunia amplexicaulis: an unusual selenium hyperaccumulator

The Fabaceae species *Neptunia amplexicaulis* (or 'Selenium Weed') is a Se hyperaccumulator occurring in the seleniferous region of Richmond, in north-west Queensland, Australia (Knott and McCray, 1959; McCray and Hurwood, 1963). It is an endemic herbaceous legume which can accumulate over 4000 μg Se g^{-1} DW when growing in soils with of up to 69 mg Se kg^{-1}, derived from Se enriched limestone and shale (Knott and McCray, 1959; McCray and Hurwood, 1963). The highest concentrations of Se in *N. amplexicaulis* are found in the developing young leaf and root tissues and reproductive tissues, which, when grown in hydroponics cultivation, can accumulate up to 13,600 μg Se g^{-1} DW in the young leaves (Harvey et al., 2020). The closely related non-accumulator *Neptunia heliophila* (formerly *N. gracilis* in Harvey et al., 2020; Pinto Irish et al., 2021) has been observed growing in the same seleniferous habitat as *N. amplexicaulis* and can be used as a comparison species (Harvey et al., 2024)

Early research into the Se chemical speciation of *N. amplexicaulis* by Peterson and Butler (1967) found Se in ethanol soluble compounds, with 90% of Se concentrated as a neutral amino acid. The authors used paper chromatography, electrophoresis, and ion exchange chromatography to identify SeCT as the main Se species present in the plant; however, two thirds of the Se amino acids extracted remained unidentified. Selenocystathionine has since been identified as a major Se species in *N. amplexicaulis* seeds (Peterson and Robinson, 1972). MeSeCys, despite being common in other Se hyperaccumulators, was not identified in *N. amplexicaulis* in these studies (Peterson and Butler, 1967; Burnell, 1981).

Selenocystathionine is the seleniferous analogue of the amino acid cystathionine, produced during a rate limiting step of the metabolism of SeCys to SeMet (Van Huysen et al., 2003). Peterson and Robinson (1972) similarly used chromatographic methods to investigate and establish the presence of cystathionine in *N. amplexicaulis*, and that there was very high selenocystathionine to cystathionine ratio compared to what was expected from other species (Peterson and Robinson, 1972). Peterson and Butler (1967) had hypothesised that SeCT was enzymatically discriminated against when forming Cys or Met, but further research did not support this hypothesis (Ng and Anderson, 1978; Dawson and Anderson, 1989). It was established that there was no measured difference in cysteine synthases (catalysing the formation of Cys or SeCys) and cystathionine-γ-synthases (for SeCT or cystathionine formation) purified from *N. amplexicaulis,* other accumulators and non-accumulators, thus seleniferous and non-seleniferous amino acid formation was catalysed by the same enzyme. However, these enzymes in both accumulators and non-accumulators displayed a greater affinity for Se over S. It should be noted that later studies showed that transcription of enzymes associated with sulphate and selenate metabolism were higher in hyperaccumulators compared to non-accumulators, however this was not confirmed for *N. amplexicaulis* specifically (Freeman et al., 2010).

1.3. Recent advances in Neptunia amplexicaulis selenium biochemistry

Given that two thirds of extracted seleno-amino acids remained unidentified by Peterson and Butler (1967), a significant part of the Se biochemistry puzzle was still missing. Burnell, in his 1981 review, noted that the pathway for MeSeCys formation was theoretically still possible in *N. amplexicaulis*, and that the lack of detectable MeSeCys was unusual when compared with other hyperaccumulators. In a more recent study, synchrotron-X-ray Absorption Spectroscopy (XAS) and Liquid Chromatography Tandem Mass Spectrometry (LC-MS) were used to identify the Se compounds in silica-dried plant material of *N. amplexicaulis,* and the compounds were fitted as MeSeCys and SeMet (Harvey et al., 2020). However, it was difficult to distinguish between C-Se-C compounds (leading to fitting MeSeCys), SeCT was not available as a standard for the LC-MS, and silica-drying plants was not ideal sample preparation for these analyses; and as such, the possibility of SeCT presence and ambiguity of the seleno-compound identification was not confirmed.

The benefit of synchrotron XAS is that it allows for *in situ* investigation of Se-complexes in plant material samples with minimal preparation. XANES spectra can detect small differences in Se compounds *(e.g.* the different protonation states of inorganic Se oxoanions are readily distinguished), which allows for linear combination fitting of mixtures of Se compounds found in biological samples (Weekley et al., 2013;

Weekley and Harris, 2013). Organic Se species containing a selenoether functionality are difficult to distinguish using XAS, but when coupled with the more organic-Se sensitive technique of LC-MS, a broad spectrum analysis of seleno-compounds present in plant tissues may be achieved. Performing this analysis on the different tissues of live hydrated material of *N. amplexicaulis* and *N. heliophila* may help resolve recent debate from preliminary analysis of silica-dried material contradicting older, purely chromatographic analytical results, and develop further context for Se metabolism in non-accumulators.

1.4. Practical uses of plant-extracted selenium for biofortification

Selenium in humans and animals helps to prevent tissue damage caused by free radicals, and Se supplementation serves as an antioxidant with anti-inflammatory and anti-viral activities (Papp et al., 2007). Selenium also has anti-metastatic properties in addition to being a cancer preventative agent in some instances (Zeng and Combs, 2008; Chen et al., 2013). The Cancer Council supports the recommendation of >50 and < 100 μg per day intake of Se, and many supplements use Se-amino acid compounds for effective integration (Schrauzer, 2001). The unique ability of hyperaccumulator plants to accumulate Se and synthesise organic compounds could be used as a technique to supplement Se, particularly in areas where dietary Se may be hard to access normally, or be used to accumulate and remove toxic concentrations of Se from the environment (Zhao and McGrath, 2009; Dhillon and Bañuelos, 2017; Schiavon and Pilon-Smits, 2017b). With appropriate knowledge of the Se compounds synthesised by plants, and extractive technologies in place, hyperaccumulators may provide a natural, alternative approach to produce pharmaceutically valuable Se compounds, or an effective source of crop Se-biofortification.

In this study, we use a combination of synchrotron X-ray fluorescence Microscopy (XFM) & XAS and LC-Tandem MS to examine the distribution and speciation of Se in *N. amplexicaulis* and *N. heliophila*. In particular, the LC-Tandem MS analysis was undertaken to add value to the XAS analysis to provide further evidence of the presence of Se-organo species in plant water extracts. The study findings will enable a better understanding of the mechanism(s) of Se tolerance in plant species for potential biofortification, bioremediation and pharmaceutical applications.

2. Materials and methods

2.1. Seed collection and culture conditions

The seeds were sourced from *Neptunia amplexicaulis* and *N. heliophila* growing in the natural habitat at Silver Hills Station near Richmond, Queensland (20.648359°S, 143.098375°E). Seeds were pricked with a scalpel and left in DI water for 24 h to germinate, then transferred to a mixture of 50% fine perlite and 50% vermiculite for one week to establish as seedlings. Seedlings were transferred to alkaline sandy soil from the University of Queensland St Lucia Campus in 10 cm pots, with two seedlings per replicate pot. Soils had been dried, sieved to 2 mm, and hydrated with DI water before being dosed: (i) a Se-deficient treatment with no added Se (control treatment), (ii) a low Se treatment (10 mg Se kg^{-1}); and iii) a high Se treatment (60 mg Se kg^{-1}), as indicated by previous dosing experiments with this species (Harvey et al., unpublished). Selenium was provided in the forms of either sodium selenate (Na_2SeO_4) or sodium selenite (Na_2SeO_3) dissolved in DI water prior to spiking. Plants were moved to an evaporative-cooled glasshouse, watered regularly and monitored for period of 7 weeks to ensure healthy growth. The plants were transported to the Australian Synchrotron (Clayton, Victoria) while still in their pots, packaged to minimise soil disruption and stem damage. After XFM and XAS analysis at the Australian Synchrotron, plants were divided into fine roots, taproot, stem, old leaves, and young leaves, dried at 60 °C in an oven and analysed for total Se.

2.2. Hydroponic culturing conditions of Neptunia amplexicaulis plants

Using the same germination protocols as used for the soil-grown plants, established seedlings were transferred to rectangular containers (11 cm height × 30 cm width × 40 cm length; 11 L each with 8 × foam baskets for individual plants) filled with Aqua Vega Classic nutrient solution (Canna, Brisbane QLD, Australia) diluted as 10 mL each of A and B solutions to 11 L DI water (~half strength), in addition to 3 mL of 20 mM FKHBED (Iron N,N′-bis (2-hydroxybenzyl)ethylenediamine-N,N′-diacetic acid) solution. The final diluted solution contained: 1.31 mM N, 0.51 mM P, 2.88 mM K, 0.43 mM Ca, 0.34 mM Mg, 0.31 mM S, 0.61 μM Fe-DTPA, 0.44 μM Fe-EDDHA, 5.45 μM FeHBED, 10 μM B, 0.14 μM Cu, 3.3 μM Mn, 0.2 μM Mn-DTPA, 0.28 μM Mo, and 1.53 μM Zn. The solution was kept constantly aerated using a 25 cm long air stone at the bottom of each container. The hydroponics solutions were spiked with sodium selenate to achieve 250 μM Se for synchrotron XFM samples (to achieve exceptional, rapid uptake of Se), 75 μM Se as sodium selenate or sodium selenite for the synchrotron XANES samples, and either 30 μM (low, stable uptake) or 150 μM Se (high uptake) as an equimolar Se ratio of sodium selenate and sodium selenite for both *N. amplexicaulis* and *N. heliophila* for HPLC-ICP-MS and LC-MS samples.

2.3. Bulk chemical analysis of samples of Neptunia amplexicaulis plants

Dried plant organ samples were ground to a fine powder with an impact mill at 19,000 rpm (Tube Mill 100 control with disposable blades). Approximately 100 mg of sample was weighed into 6 mL polypropylene tubes. Where samples were too small to grind, whole organs were weighed up to 100 mg in 6 mL polypropylene tubes. These samples were pre-digested using 2 mL (or 1 mL for 50 mg) concentrated nitric acid (HNO_3,70%, Ajax finechem AR-grade) for 24 h before being open vessel block digested (Thermo Scientific™ digital dry bath) for 2 h (1 h at 70 °C followed by 1 h at 125 °C) and diluted to 10 mL with ultrapure water (Millipore 18.2 MΩ cm at 25 °C). Plant digest solutions were analysed for metals and metalloids using inductively coupled plasma - atomic emission spectroscopy (ICP-AES) (Thermo Scientific iCAP 7400) in radial and axial modes depending on the element and expected analyte concentration (measured for Na, Mg, K, Ca, P, S, Fe, Mn, Cu, Zn, Mo, V and Se). All elements were calibrated with a 4-point curve covering analyte ranges in the samples. In-line internal addition standardization using yttrium was used to compensate for matrix-based interferences. Quality controls included matrix blanks, TraceCERT (Sigma-Aldrich) certified reference material for calibrations, Standard Reference Material (NIST Apple 1515) and *Neptunia amplexicaulis* amalgamated reference material (Suppl. Tables 1 and 2).

2.4. Synchrotron investigations for distribution and chemical speciation of selenium

A synchrotron is a particle accelerator that uses electrons to generate powerful X-rays, which can then be used for a multitude of different analytical techniques. Synchrotron X-ray fluorescence microscopy (XFM) is a technique that allows for the mapping of elemental distribution within a sample, in this case the prevailing concentrations of K, Ca, Se and Br in fresh hydrated plant tissues. The Australian Synchrotron XFM beamline directs X-rays at a given specimen using a Si(111) monochromator and a pair of Kirkpatrick-Baez mirrors. Fluorescent X-rays are collected in a backscatter geometry using the 384-element Maia detector system, which uses a large detector array for efficient imaging (Lombi et al., 2011; Paterson et al., 2011). Maia enables high overall count-rates and uses an annular detector geometry, where the beam passes through the detector and strikes the sample at normal incidence, enabling large solid angle (1.2 steradians) to be collected in order to either maximise detected signal or to reduce the dose and potential damage to a specimen (Kirkham et al., 2010; Siddons et al., 2014; Ryan

et al., 2010, 2018). Radiation-induced damage to fresh hydrated tissues was taken into account, as fresh plant tissue has a dose-limit up to 4.1 kGy before detectable damage occurs, so radiation damage was limited by utilising fast scanning (per-pixel dwell time is less than 10 ms) (van der Ent et al., 2018; Jones et al., 2019). The samples were held between two sheets of polyethylene (Ultralene) thin film (4 μm) stretched over a Perspex frame to prevent de-hydration duration the measurement.

Selenium K-edge X-ray absorption near edge spectroscopy (XANES) mapping of live *Neptunia amplexicaulis* were recorded at the Australian Synchrotron on the XFM beamline with the same beamline configuration as described above for the XFM analysis. XANES mapping allows for the spatially resolved elucidation of chemical species of Se within a fresh hydrated plant sample. This is achieved by analysing the sample with multiple X-ray energies sequentially (over the K-edge of the target element) and observing differences in the absorption across these energies. XANES maps consist of a hyperspectral stack of μXRF maps of a series of 112 energies across the Se K-edge with a 10 ms/energy dwell time. The following energy ranges were used for XANES data collection: pre-edge region from 12,605 to 12,645 eV (10 eV steps), 12,645 to 12,650 (1 eV steps), 12,650 to 12,675 eV (0.5 eV steps), 12,675 to 12,684 eV (1 eV steps), 12,684 to 12,700 eV (4 eV steps), 12,700 to 12,740 eV (5 eV steps) and 12,740 to 12,860 eV (10 eV steps). Due to the duration required to complete data collection, XANES imaging was conducted on single plants dosed with either SeO_4^{2-} (75 μM) or SeO_3^{2-} (75 μM). X-ray absorption spectroscopy (XAS) uses specifically tuned X-rays to excite the target elements within bulk samples and analyse the differences in absorption spectra to identify the chemical forms of that element in a sample. Bulk XAS is more sensitive and accurate than XANES mapping, but lacks the spatial component. The XAS beamline at the Australian Synchrotron was used to collect X-ray absorption near edge structure (XANES) spectra of plant tissue; the methods as follows are from the same beamtime session detailed in Harvey et al. (2024). Fresh hydrated plant tissue samples were inserted in plastic cells, sealed in Kapton tape, and cooled to ~5 K in a He expansion cryostat. XAS spectra of the samples were recorded in fluorescence mode using a 100-element solid-state Ge fluorescence detector array at 90° to the incident beam. The energy ranges to be utilised for XANES Se-edge data collection are pre-edge region 12,430–12,635 eV (10 eV steps); XANES region 12,635–12,685 eV (0.25 eV steps); post-edge region 12,685–12,875 eV. A spectrum of a hexagonal elemental $Se_{(s)}$ standard, recorded simultaneously in transmission downstream of the sample, was used to calibrate the energy scale to the first peak of the first derivative of the elemental Se edge (12,658.0 eV). Spectra of model Se compounds, as previously reported, for target transformation analysis and XANES linear combination fitting were (abbreviations used in tables and figures in parentheses): aqueous selenate at pH 7 (selenate pH7), aqueous selenite at pH 5 and 7 (selenite pH5, selenite pH7), seleno-L-cystine (CysSeSeCys), sulphoseleno-L-cystine (CysSSeCys), seleno-L-methionine (SeMet), Se-methylselenocysteine (MeSeCys), selenodiglutathione (GSSeSG), protonated and deprotonated seleno-L-cysteine (CysSeH and $CysSe^-$) and, dimethyl selenoxide (DMSeO) (Weekley et al., 2013, 2014). Standards for selenocystathionine (SeCT) were not available. The following spectral models were also considered but not identified as significant by target transformation and not included in linear combination fitting; elemental Se (solid red allotrope), dimethyl selenone, aqueous selenite at pH 12 and the hydrogen selenide anion (HSe^-).

2.5. Liquid chromatography mass spectrometry analysis of chemical speciation of selenium

These techniques employ chromatographic methods to elucidate organic compounds in plant extracts, used here to identify the organic selenium compounds present in extracts of *N. amplexicaulis* and *N. heliophila* plant tissue. Powder plant material from two hydroponically grown *N. amplexicaulis* and *N. heliophila* plants were combined and freeze-dried to a constant mass. The freeze-dried samples were homogenised into a powder using a stainless-steel grinder. Approximately 0.1 g of the plant powders (*N. amplexicaulis* and *N. heliophila)* were weighted into 15 ml centrifuge tubes and 2 ml of ultrapure deionised water (Milli-Q, Millipore) was added. The samples were sonicated in an ultrasonic water bath for 45 min at 25 °C. After sonication the samples were centrifuged at 3000 rpm for 30 min and the supernatants removed. Approximately 2 ml of the sample supernatants were ultracentrifuged using 10 kDa MWCO devices (Microsep) at 4000 rpm for 60 min. The <10 kDa sample filtrates were analysed for Se compounds by Liquid Chromatography-Tandem Mass Spectrometry. A SCIEX ExionLC AD autosampler with column oven, LC pumps and degasser (SCIEX, MA USA) were used for liquid Chromatography (LC) separation. Waters Atlantis column 5μ dC18 column (150 × 2.1 mm) was used with a binary mobile phase, a mixture of 0.1% formic acid with 10 mM ammonium formate and methanol, at a flow rate of 0.25 mL/min (total run = 20 min). The column oven and the autosampler temperature were set at 30 °C and 10 °C, respectively. The sample volume injected was 20 mL. An AB SCIEX TripleTOF™ 5600+ system (SCIEX, MA USA) with electrospray ionisation (ESI) positive mode was used for the identification of Se compounds in samples. The time of flight-mass spectrometry (TOF-MS) was calibrated with an ESI positive calibration solution for each sample. Specific positive charged Se compounds were targeted with multiple reaction monitoring (MRM) (Suppl. Table 3). The collision cell was set at collision energy (CE) 35V with collision energy spread (CES) ±15 V. The resolution of TOF-MS spectra was >32,000 (FWHM), the accurate mass was scanned between 100 and 900 m/z. The MS/MS spectra was >15,000 (FWHM). The data were processed with MasterView. We recognise the LC-Tandem Mass spectrometry analysis undertaken in this study would not provide a comprehensive profile of Se species in the <10 kDa water extracts. The use of complementary techniques such as high-performance liquid chromatography (*i.e.,* ion exchange, revere phase)-inductively coupled plasma-mass spectrometry, and high/ultra high-resolution mass spectrometry techniques under different ionisation conditions (*e.g.,* TOF-MS, Orbitrap mass spectrometry, and/or Fourier Transform Ion Cyclotron Resonance Mass Spectrometry) would be needed to provide a comprehensive understanding of the unique composition and concentrations of Se species in these samples. Total Se concentrations in plant powders (*Neptunia amplexicaulis* and *Neptunia heliophila)* used for LC-tandem-MS analysis were determined following concentrated nitric acid closed vessel microwave digestion (US EPA method 3051A, 1998). Sample solutions following digestion and <10 kDa water extracts were analysed for total Se concentrations, following appropriate dilution using ultrapure deionised water, using triple quadrupole inductively coupled plasma-mass spectrometry (Agilent 8800).

2.6. Data analysis

The XRF event stream was analysed using the Dynamic Analysis method as implemented in GeoPIXE (Ryan et al., 1990; Ryan and Jamieson, 1993; Ryan, 2000). This method generates elemental images, which are (i) overlap-resolved, (ii) with subtracted background and (iii) quantitative, *i.e.,* in μg g^{-1} dry weight units. Spatial XANES spectra integrated across different plant anatomical regions were generated for each plant using the MANTiS software (Lerotic et al., 2014). Selenium species distribution maps were generated by fitting spectra of model Se compounds within the MANTiS software. Image processing of the distribution maps was completed in ImageJ (Schneider et al., 2012). Spectral analysis including calibration, averaging, background subtraction and linear combination fits were performed on average spectra from ROI using EXAFSPAK software package in accordance with previously reported procedures (G. N. George, Stanford Synchrotron Radiation Laboratory, Stanford, CA). Linear combination fits of model Se compounds to plant XANES spectra were performed between 12,605 eV and 12,750 eV region. The model library was comprised of elemental Se, SeMet, MeSeCys, selenite and selenate and were collected at the

Australian Synchrotron XFM beamline with identical energy ranges as described above for the plant images. The elemental Se model was prepared by *in situ* reduction on a filter paper wetted with a solution of sodium selenite using a solution of sodium ascorbate, followed by air drying. The remaining models were prepared by drying aqueous solutions of the respective compounds on filter paper. Due to spectral resolution of the XANES imaging, SeMet and MeSeCys could not be confidently distinguished, thus, the SeMet model spectrum was utilised for spectral fits and represents total organic Se.

The XAS data was interpreted with standard approaches using EXAFSPAK. All data was energy calibrated, background corrected and normalized. Each set of non-spatial XANES data were subjected to a principal component analysis, then the significance of each of the set of 15 model spectra for each sample set was assessed using a target transformation against the output of the respective principal component analysis. The top-ranked models for each set were then fit to the sample spectra from each set using a linear combination approach, with the number of models included defined by the principal component analyses. Components with a fit fraction less than three times the estimated standard deviation for that parameter were excluded.

3. Results

3.1. Selenium concentrations in experimental N. amplexicaulis plants

Old leaves across every treatment had the lowest Se concentrations of any tissue, whilst the highest values were in the taproots and fine roots, reaching up to 16,300 μg g^{-1} Se (Table 1). In the low and high Se treatments, tissues exposed to selenate were consistently higher in Se concentrations than the equivalent tissues from plants exposed to selenite.

3.2. Elemental distribution in Neptunia amplexicaulis tissues

In the roots of Se dosed plants, Se was most concentrated in the pericycle, and the secondary xylem tissue directly surrounding the primary xylem, with >10,000 μg Se g^{-1} in these tissues. This is displayed in the maps of elemental concentrations in sections of plant tissues (XFM GeoPIXE map scales) (Fig. 1.). Calcium was more concentrated in the remnant cortex, primary xylem, and phloem channels. In the stems, Se was relatively more concentrated in the younger stem than the basal stem, and occurred primarily in the epidermis and cortex, cambium, and xylem tissues (Fig. 2). Potassium was mostly localised in the cortex, residual procambium and protoxylem tissues, and in the pith of the basal stems. Calcium occurs at the edges of the cortex and in the epidermis and was more concentrated in the ridges of the stems, and phloem tissues. In the younger stems, Ca also occurs in sections of the metaxylem. Selenium was concentrated in the veins of the fully developed, younger leaflets, particularly towards the basal ends of the leaflets, and around the leaf margin (Fig. 3). Selenium is lower in the lamina and pulvinus and not detectable in the trichomes. Apical leaflets of a pinna have a less distinct distribution of Se through the veins, but Se also occurs in higher concentrations at the apical ends of the rachis (Fig. 4). Potassium is concentrated in the rachis and pulvini and is also present throughout the lamina and apical veins (Fig. 3). The basal veins had very low K. Calcium occurred as small deposits occurring in a regular pattern, with the highest density and concentrations occurring in the veins, particularly towards the apical ends of the veins (Figs. 3 and 4). Moderately concentrated and heterogeneously distributed deposits of Ca occur throughout the lamina with very little present in the pulvini, leaf margin or trichomes. Calcium was present in the rachis.

Table 1
Selenium concentration averages (μg Se g^{-1} dry weight) of organs of the *N. amplexicaulis* samples used for XAS[a].

Se Form	Soil Se (mg kg^{-1})[b]	*n*	Young leaf	Old leaf	Stem	Taproot	Fine root
control	0	5	82	14	41	49	42
SeO_4^{2-}	10	1	2136	136	1538	1567	2595
SeO_4^{2-}	60	2	4726	421	6248	11714	16246
SeO_3^{2-}	10	2	381	46	303	399	820
SeO_3^{2-}	60	2	1201	124	1701	2762	3008

[a] Plant concentrations as the average of number of available specimens.
[b] soil Se dosed as low (10 mg Se kg^{-1}) and high (60 mg Se kg^{-1}) in the form of Na_2SeO_4 or Na_2SeO_3.

3.3. Selenium chemical speciation and distribution in Neptunia amplexicaulis: spatial XANES

XANES imaging over the Se K absorption edge was conducted on live *N. amplexicaulis* plants with either SeO_4^{2-} or SeO_3^{2-} exposure to assess differences in Se chemical speciation and distribution (Fig. 5; Suppl. Fig. 1–4; Table 2). Maps show the differences in Se chemical speciation in plant samples to assess components of Se forms in the whole specimens or at different points (*i.e.* different organs and tissues) of the same sample. Linear combination fitting of the total average of both the SeO_4^{2-} (75 μM) and SeO_3^{2-} (75 μM) exposed plants, shows that organic-Se is the predominant form of Se in both (Table 2). Similarly, SeO_4^{2-} and SeO_3^{2-} exposed plants had similar proportions of total Se comprised of elemental Se with 25 ± 1.0% and 28.7 ± 0.9% respectively. The major difference in chemical speciation was that the SeO_4^{2-} dosed plant contained ~3-fold higher proportion of SeO_4^{2-} at 9.4 ± 0.4% compared to 3.1 ± 0.4% observed in the SeO_3^{2-} dosed plant. Neither the SeO_4^{2-} nor SeO_3^{2-} dosed plants had detectable SeO_3^{2-} (Table 2). Fig. 5 shows the Se chemical speciation distribution maps for both the SeO_4^{2-} and SeO_3^{2-} exposed plants; maps produced using MANTiS were validated though linear combination fitting using EXAFSPAK (Suppl. Table 4). The SeO_4^{2-} dosed plant had higher SeO_4^{2-} in all anatomical regions compared to the SeO_3^{2-} dosed plant counterpart, with the highest concentration observed in the stipels (Fig. 5a–Table 2). The selenite dosed plant did not have any significant proportion of SeO_3^{2-}, suggesting that there was either no increase in SeO_3^{2-} absorption by the plant or rapid conversion into other Se species. The XANES maps also reveal differences in SeO_4^{2-} distribution in the leaves of plants exposed to SeO_4^{2-} and SeO_3^{2-} (Suppl. Table 5, Suppl. Fig. 1). The tips of mature leaves of the SeO_4^{2-} dosed plant contained an approximately twofold higher proportion of SeO_4^{2-} compared to the base of the leaves (29.1 ± 0.5% compared to 14.3 ± 0.4%) potentially associated with Se volatilization. This was not evident in the young leaves from the SeO_4^{2-} dosed plant nor within the leaves of the SeO_3^{2-} dosed plant (Table 2).

3.4. Selenium chemical speciation in N. amplexicaulis plant organs: synchrotron XAS analysis

X-ray absorption spectroscopy at the Se K absorption edge of bulk, intact *N. amplexicaulis* organs was conducted to examine the differences in Se chemical speciation within different plant organs. The results of linear combination fitting of XANES spectra of a selection of model Se compounds (Suppl. Fig. 5) to the plant tissues are shown in Tables 3–5 and the spectra of the samples are depicted in Figs. 6–8. The study found significant changes in the edge spectra from the lower dosing concentration samples as a function of beam exposure time and, in these cases, our analyses were conducted on only the first scan on a particular sample location in an effort to minimise photodamage artefacts. All sample spectral fits were dominated by a contribution from either the model Se-methyl selenocysteine or the selenomethionine spectra, or a combination of the two. These model spectra share a “white line” peak energy of ~12,661 eV, consistent with the sample spectra, as well as a significant higher energy peak at ~12,667 eV. The edge spectra of the two selenoether amino acids (SeMet and MeSeCys) can be difficult to distinguish and are apparently sensitive to exact microenvironmental conditions such as pH and concentration. This sensitivity also means

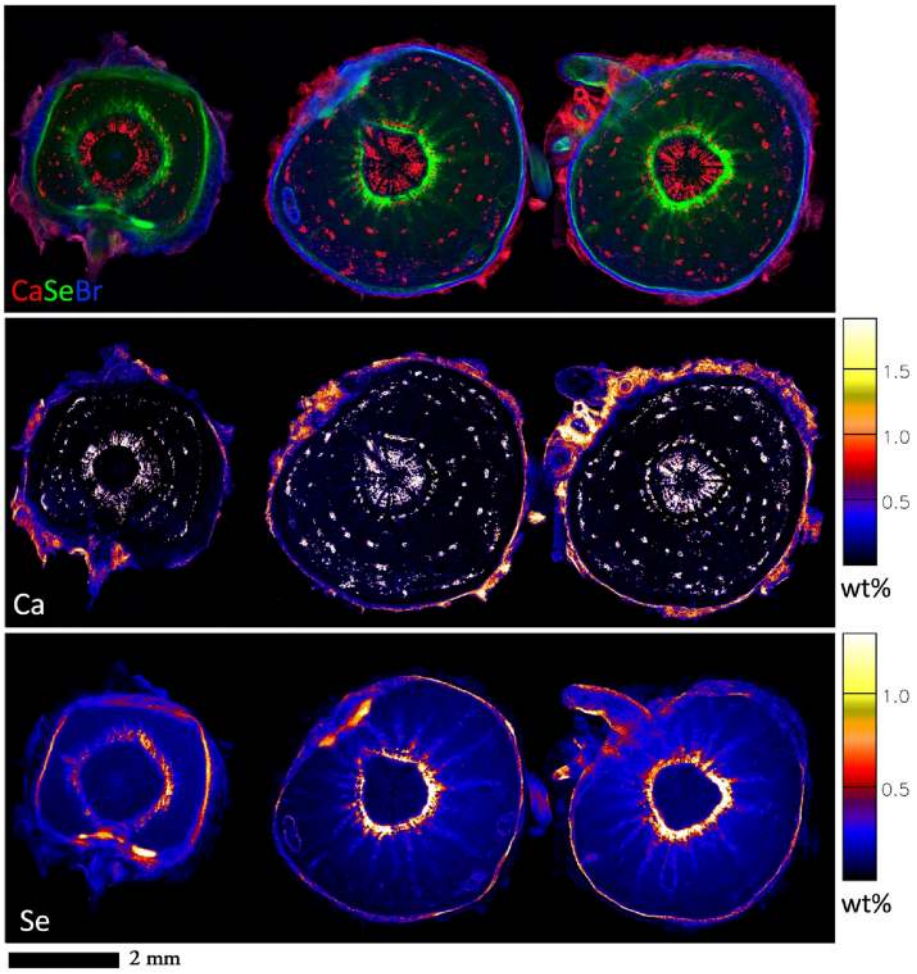

Fig. 1. Synchrotron XFM elemental maps of K, Ca, and Se of hydrated root cross-sections of *Neptunia amplexicaulis* grown in a glasshouse in sandy soil spiked with 28 μg Se g^{-1} as sodium selenate. Scale bar denotes 2 mm, Ca and Se concentrations shown in weight percent. The tricolour image on the top has been shown in our review (Pinto Irish et al., 2023) used under CC BY 4.0 license here.

that despite the similarity of their chemical structures, they cannot serve as perfect models for other related Se containing amino acids, such as selenocystathionine. The variation in the relative fitted contributions of Se-methyl selenocysteine and selenomethione should not be interpreted as robust – rather the sum of the two component fraction may be considered as an estimate of the fraction of selenoether forms present in a sample. Nonetheless, the XANES fitting results, taken over all and identifying an organic selenoether as the dominant species present in the plant samples, are consistent with the LC-MS/MS analysis of selenocystathionine (which is a selenoether) as the main water extractable Se species identified form *N. amplexicaulis*.

Selenate was identified as a minor species present in some stem and especially root organs. The XANES spectrum of aqueous selenate at neutral pH has an extremely intense white line peak at 12,667.3 eV and even though this is coincident with the second peak of the selenoether forms, the presence of selenate in speciation mixtures is reliably identified with good sensitivity by an increase of the relative intensity ratio of the two peaks (high E:low E), and because there are no other biologically relevant Se(VI) compounds which could give rise to a peak at the higher energy. This variations in peak height ratio can be found in Fig. 6 (Table 3). We note that other model compound spectra are identified as minor contributing components to the XANES fits of some samples, in particular dimethyl selenoxide, selenite ion, selenocystine and sulphoselenocystine. However, given the uncertainty arising from the lack of a certified model spectrum of selenocystathionine and some evidence for beam photodamage noted above, further analyses and corroboration would be required to unambiguously demonstrate the presence of these species. We hypothesise that the selenocystine model actually represents elemental Se present on the outside of root tissues given the observation that roots of *N. amplexicaulis* grown in soil are occasionally red in colour to the naked eye and we note that this species would not be detected by standard LC procedures. We suggest that, due to their size and composition, these accumulations of elemental Se may be subject to the known XAS artefact of self-absorption and hence not accurately fit by the model compound spectrum used in the analysis for red elemental Se.

3.5. Selenium chemical speciation in plant organs: HPLC-ICP-MS and LC-tandem MS

Chromatographic techniques were employed to analyse the different organic forms of Se in both plant species. The *N. amplexicaulis* plant material contained 1037 μg Se g^{-1} whilst *N. heliophila* contained 208 μg Se g^{-1}. The total Se in <10 kDa water extracts was 563 μg Se g^{-1} and 84 μg Se g^{-1} for *N. amplexicaulis* and *N. heliophila*, respectively. Mass spectra examples for the <10 kDa water extracts from *N. amplexicaulis* and *N. heliophila* by LC-tandem MS can be found in Supplementary Material Figs. 6, 7 and 8. The mass spectra obtained were very noisy but regions with the observable Se-isotopic pattern could be identified in samples. For *N. amplexicaulis* <10 kDa water extracts, a relatively strong intensity (signal) with natural Se-isotopic pattern could be identified at mass of m/z = 271.0193 (Suppl. Fig. 6). Relatively smaller intensities with a natural Se-isotopic pattern

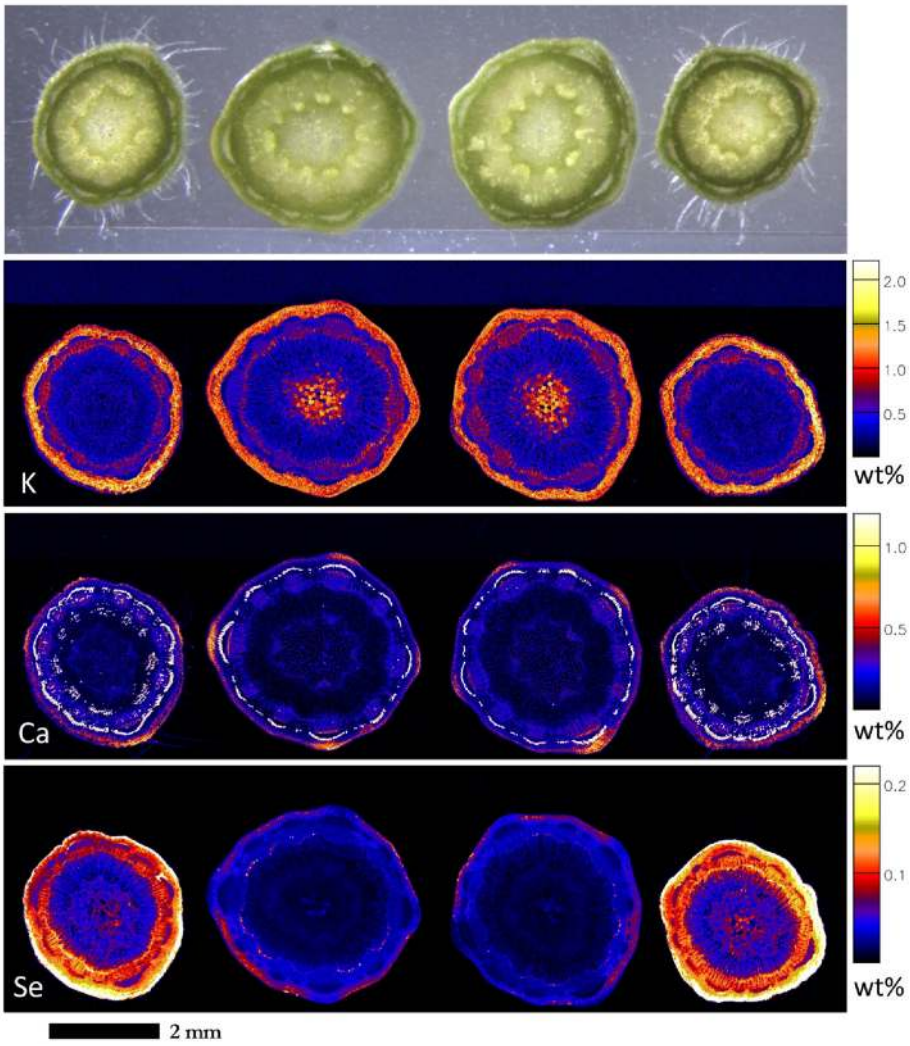

Fig. 2. Synchrotron XFM elemental maps of K, Ca, and Se hydrated stem cross-sections of *Neptunia amplexicaulis* grown in glasshouse in sandy soil spiked with 28 μg Se g^{-1} as sodium selenate. Scale bar denotes 2 mm, K, Ca and Se concentrations shown in weight percent.

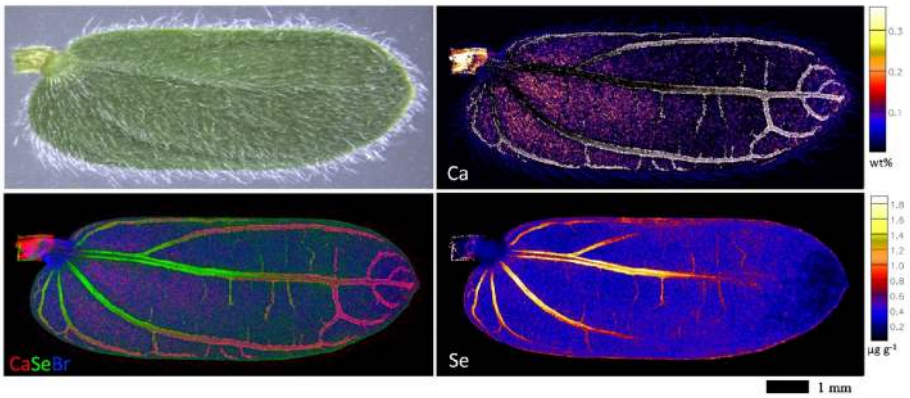

Fig. 3. Synchrotron XFM elemental maps of K, Ca, and Se of a hydrated whole leaflet of *Neptunia amplexicaulis* grown in glasshouse in sandy soil spiked with 28 μg Se g^{-1} as sodium selenate. Scale bar denotes 1 mm, Ca concentrations shown in weight percent, Se concentrations shown in μg Se g^{-1}.

could be identified at mass of m/z = 400.0688, m/z = 181.9710 (Suppl. Fig. 7), m/z = 166.9593, and m/z = 135.9659. The relatively strong signal with natural Se-isotopic pattern at mass of m/z = 271.0190 may be attributed to the presence of selenocystathionine ($[C_7H_{14}N_2O_4Se + H]^+$, ^{80}Se) in <10 kDa water extracts (Montes-Bayón et al., 2002; Dernovics et al., 2007). Selenocystathionine has previously been found in *N. amplexicaulis* through different techniques (Peterson and Butler, 1967). The presence in mass spectrum of Se compounds at m/z = 181.9710 ($[C_4H_7NO_2Se + H]^+$ or $[C_4H_8NO_2Se^+]$, ^{80}Se), m/z = 166.9593 ($[C_4H_7O_2Se^+]$, ^{80}Se) and m/z = 135.9659 ($[CH_3H_6NSe^+$ or $CH_3H_5NSe +$

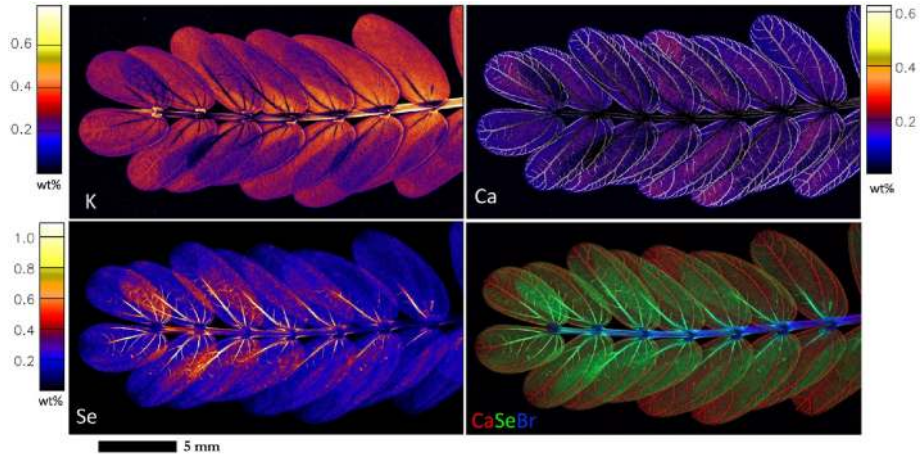

Fig. 4. Synchrotron XFM elemental maps of K, Ca, and Se of a hydrated whole young pinna *Neptunia amplexicaulis* grown in glasshouse in sandy soil spiked with 28 μg Se g^{-1} as sodium selenate. Scale bar denotes 5 mm, K, Ca and Se concentrations shown in weight percent. The tricolour image on the bottom right has been shown in our review (Pinto Irish et al., 2023) used under CC BY 4.0 license here.

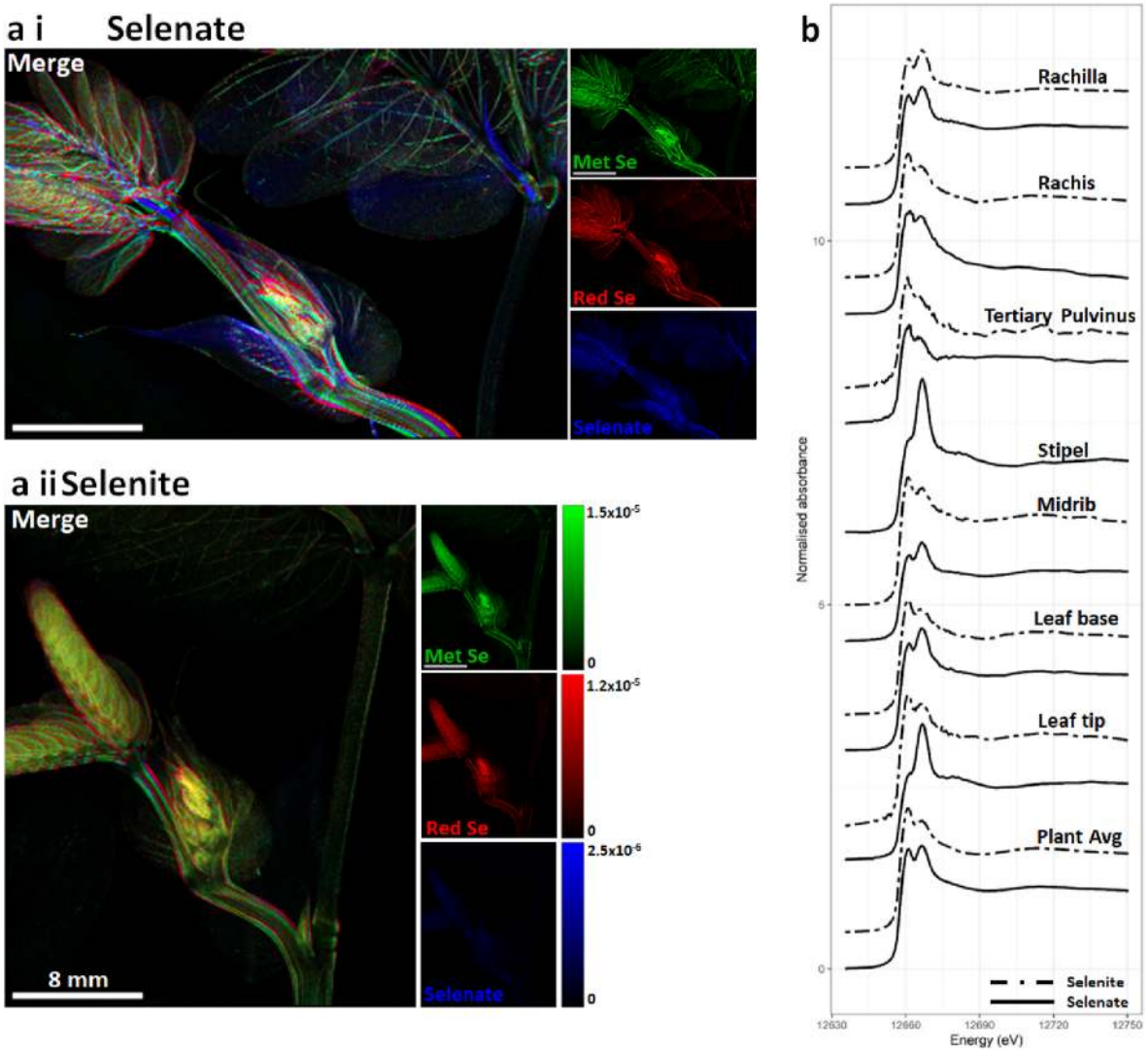

Fig. 5. Selenium species distribution in hydrated leaf and stem portion of *N. amplexicaulis*. **ai** plants supplied with selenate (75 μM), **aii** plants supplied with selenite (75 μM). **b** Se K-edge of normalized XANES spectra from multiple plant regions from plants hydroponically supplied with selenite (dashed traces) or selenate (solid traces). Scale bars denotes 8 mm.

Table 2
Selenium chemical speciation proportions in multiple regions of *N. amplexicaulis* hydroponically supplied either Selenate (75 μM) or Selenite (75 μM) as estimated by linear combination fitting of model spectra. Reported as detected Se species as proportion of total Se.

ROI	SeMet	Selenate	Elemental Se	Residuals	Organic	Inorganic
Whole selenate plant average	65.4% (1.3%)	9.4% (0.4%)	25.0% (1.0%)	0.057%	**65.4% (1.3%)**	**34.6% (1.4%)**
Whole selenite average plant	68.2% (1.1%)	3.1% (0.4%)	28.7% (0.9%)	0.044%	**68.2% (1.1%)**	**31.8% (1.3%)**
Selenate leaf tip	58.7% (1.7%)	29.1% (0.5%)	15.0% (1.3%)	0.085%	**58.7% (1.7%)**	**44.0% (1.8%)**
Selenite leaf tip	67.8% (1.2%)	4.9% (0.4%)	27.3% (1.0%)	0.054%	**67.8% (1.2%)**	**32.2% (1.4%)**
Selenate leaf base	65.0% (1.1%)	14.3% (0.4%)	20.7% (0.9%)	0.042%	**65.0% (1.1%)**	**35.0% (1.3%)**
Selenite leaf base	69.1% (1.2%)	3.8% (0.4%)	27.1% (1.0%)	0.049%	**69.1% (1.2%)**	**30.9% (1.4%)**
Selenate midrib	65.2% (2.3%)	13.5% (0.7%)	21.3% (1.8%)	0.124%	**65.2% (2.3%)**	**34.8% (2.5%)**
Selenite midrib	68.9% (1.1%)	3.5% (0.3%)	27.6% (0.9%)	0.039%	**68.9% (1.1%)**	**31.1% (1.2%)**
Selenate stipel	53.2% (2.8%)	33.1% (0.9%)	13.7% (2.3%)	0.319%	**53.2% (2.8%)**	**46.8% (3.2%)**
Selenite stipel (NA)	–	–	–	–	-	-
Selenate tertiary pulvinus	68.1% (2.7%)	–	31.8% (2.2%)	0.183%	**68.1% (2.7%)**	**31.9% (2.2%)**
Selenite tertiary pulvinus	63.2% (4.8%)	–	36.8% (4.6%)	1.6%	**63.2% (4.8%)**	**36.8% (4.6%)**
Selenate rachis	58.5% (1.2%)	16.6% (0.4%)	24.9% (1.0%)	0.059%	**58.5% (1.2%)**	**41.5% (1.4%)**
Selenite rachis	67.2% (1.4%)	3.0% (0.4%)	29.8% (1.1%)	0.061%	**67.2% (1.4%)**	**32.8% (1.5%)**
Selenate rachilla	64.1% (0.8%)	11.6% (0.3%)	24.3% (0.7%)	0.021%	**64.1% (0.8%)**	**35.9% (1.0%)**
Selenite rachilla	69.3% (1.7%)	4.0% (0.5%)	26.7% (1.3%)	0.084%	**69.3% (1.7%)**	**30.7% (1.8%)**

Table 3
Results of linear combination fitting of model compound spectra to Se K-edge XANES spectra of fresh *Neptunia amplexicaulis* samples grown in soil spiked with SeO_4^{2-} at 60 mg Se kg^{-1}. Refer to Materials and Methods for details regarding spectral models – DMSeO is dimethyl selenoxide; MeSeCys is aqueous Se-methyl selenocysteine; CysSSeCys is sulphoseleno-L-cystine.

Sample	proportion of model spectral component fitted				N_{tot}	residual ($\times 10^{-3}$)
	DMSeO	**MeSeCys**	**selenate pH7**	**CysSSeCys**		
Young leaf	–	1.0	–	–	1.01	6.24
Young leaf	–	1.0	–	–	1.01	5.15
Old leaf	0.05	0.97	–	–	1.02	8.72
Old leaf	–	1.0	–	–	1.01	8.47
Taproot	–	0.84	0.07	0.09	1.00	4.26

H]$^+$, ^{80}Se) may be due to the presence of fragment ions from selenocystathionine (Dernovics et al., 2007). The relatively small intensity with natural Se-isotopic pattern at mass of m/z = 400.0688 may be attributed to the presence of an isomer of γ-glutamyl- selenocystathionine (2-γ-Glutamylamino-4-(2-amino-2-carboxyethylselenyl)butyric acid or 2-Amino-4-(2-γ-glutamylamino-2-carboxyethylselenyl)butyric acid; $C_{12}H_{21}N_3O_7Se + H]^+$) (Dernovics et al., 2007).

For *Neptunia heliophila* a relatively strong intensity with a natural Se-isotopic pattern could be identified centred at mass of m/z = 166.9586 (Suppl. Fig. 8). This m/z = 166.9586 may be attributed to Se-methyl-selenocysteine minus the neutral loss of ammonia ($C_4H_7O_2Se^+$; [M + H-NH_3]$^+$, ^{80}Se) in the ESI ion source (Preud'homme et al., 2012; Shao et al., 2014). A relatively minor intensity centred at mass of m/z 183.9873, not showing the correct Se-isotopic pattern likely due to spectral noise, may be attributed to the primary ion for Se-methyl-selenocysteine [($C_4H_{10}NO_2Se^+$, [M+H]$^+$, ^{80}Se). The findings

Table 4
Results of linear combination fitting of model compound spectra to Se K-edge XANES spectra of fresh *Neptunia amplexicaulis* samples grown in soil spiked with SeO_3^{2-} at 60 mg Se kg^{-1}. Refer to Materials and Methods for details regarding spectral models– DMSeO is dimethyl selenoxide; MeSeCys is aqueous Se-methyl selenocysteine; SeMet is aqueous selenomethionine; CysSSeCys is sulphoseleno-L-cystine.

Sample	proportion of model spectral component fitted					N_{tot}	residual ($\times 10^{-3}$)
	DMSeO	MeSeCys	selenate pH7	SeMet	CysSSeCys		
Young leaf	–	0.62	0.01	0.37	–	1.01	6.63
Young leaf	–	0.66	0.02	0.34	–	1.01	9.46
Old leaf	0.09	0.92	0.02	–	–	1.02	10.1
Old leaf	0.07	0.88	0.08	–	–	1.03	8.15
Stem	0.06	0.50	0.36	–	0.08	0.99	7.80
Taproot	0.04	0.64	0.21	–	0.12	1.01	8.38
Fine root	–	0.66	0.06	–	0.29	1.01	2.71

Table 5
Results of linear combination fitting of model compound spectra to Se K-edge XANES spectra of fresh *Neptunia amplexicaulis* samples grown in hydroponic media containing 250 μM SeO_4^{2-}. Refer to Materials and Methods for details regarding spectral models - MeSeCys is aqueous Se-methyl selenocysteine; SeMet is aqueous selenomethionine; CysSSeCys is sulphoseleno-L-cystine.

Sample	proportion of model spectral component fitted					N_{tot}	residual ($\times 10^{-3}$)
	selenite pH5	MeSeCys	selenate pH7	SeMet	CysSSeCys		
Young leaf	0.02	0.91	0.02	–	0.08	1.03	6.94
Stem	0.03	0.80	0.06	–	0.16	1.04	7.60
Taproot	–	–	0.06	0.88	0.06	1.00	9.35

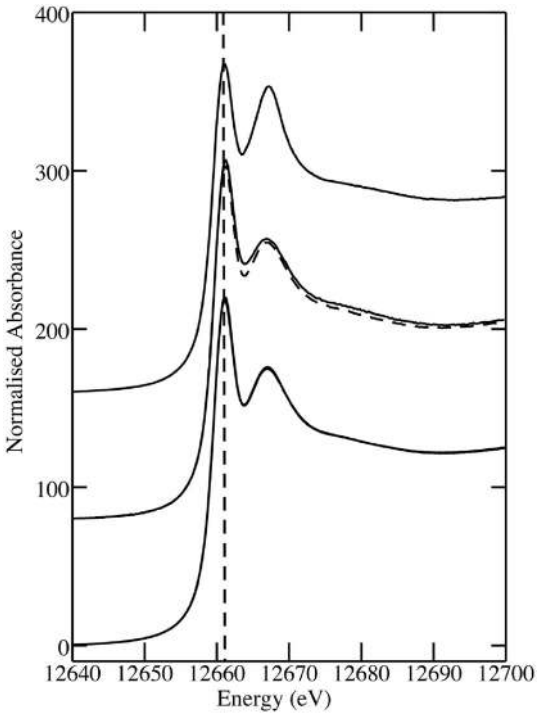

Fig. 6. Synchrotron XANES spectra *Neptunia amplexicaulis* samples grown in soil spiked with SeO_4^{2-} at 60 mg Se kg^{-1}. Spectra from top to bottom are from: Taproot, old leaf and young leaf (multiple samples overlayed).

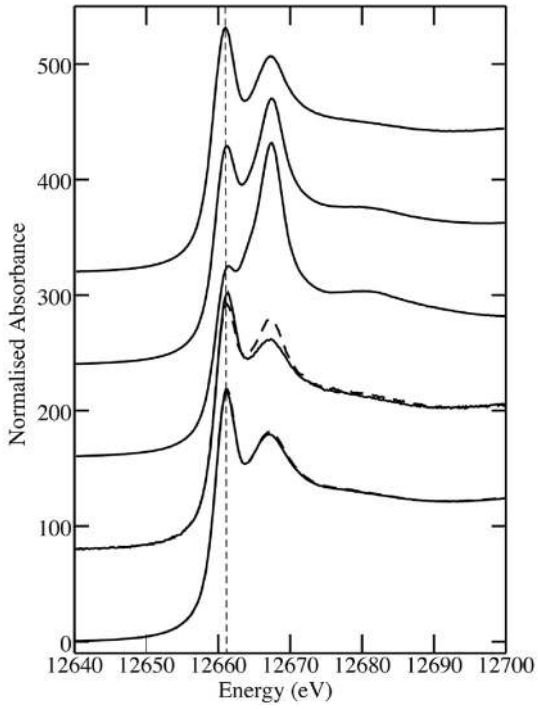

Fig. 7. Synchrotron XANES spectra *Neptunia amplexicaulis* samples grown in soil dosed with SeO_3^{2-} at 60 mg Se kg^{-1} Spectra from top to bottom are: Fine root, taproot, stem, old leaf (multiple samples overlayed) and young leaf (multiple samples overlayed).

in this study represent Se compounds that could be identified with a natural Se-isotopic pattern, that could be identified in mass spectra from *N. amplexicaulis* and *N. heliophila* water extracts. Water extracts represented ~50 % of the total Se recovered from the powdered plant

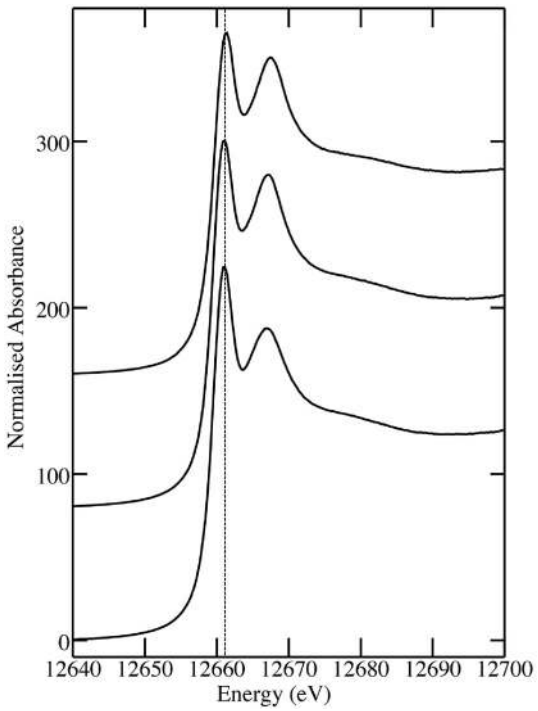

Fig. 8. Synchrotron XAS spectra *Neptunia amplexicaulis* samples grown in hydroponic media containing 250 μM SeO_4^{2-}. Spectra from top to bottom are: taproot, stem and young leaf.

samples. The water extraction method was not optimised for the *N. amplexicaulis* and *N. heliophila* so likely could be enhanced for Se water extraction.

4. Discussion

4.1. Selenocystathionine identified in water extracts from of *N. amplexicaulis*

The identification of SeCT in water extracts of *N. amplexicaulis* in this study is consistent with the findings from Peterson and Butler (1967) and to preliminary investigations aiming to identify MeSeCys in plant tissues resulting in the presence of an 'unknown compounds' (Peterson and Butler, 1961). In this study, SeCT, isoforms of SeCT and small components of γ-glutamyl Se were the only organic Se species that could be identified in water extracts, which contained only ~50% of total plant Se. Conversely, Peterson and Butler employed ethanol extraction of Se compounds and identified only ~35% of the Se amino acids extracted, with the Se speciation in the remaining fraction unknown (Peterson and Butler, 1967). Our attribution of organo-Se to SeCT is due to the high amount and proportion of this compound in the plant itself and prior standardless identification of SeCT in MS studies (Dernovics et al., 2007). In addition, synchrotron XAS, spatial XANES and preliminary LC-MS identified the presence of selenate in *N. amplexicaulis* in the current analysis, with minor proportions existing in most tissues, and more present in plants dosed with selenate compared to plants dosed with selenite.

4.2. Selenocystathionine within the metabolism model

Model pathways of Se uptake and assimilation in hyperaccumulators have been extensively discussed in the literature. Most focus is on the pathway of Se uptake into the cell, Se metabolism in the plastid and the formation of MeSeCys using the selenocysteine methyltransferase (SMT) enzyme, and eventually the formation of dimethyl-diselenide (DMDSe)

gas (Sors et al., 2005; Pilon-Smits and Quinn, 2010; Lima et al., 2018). While this model applies well to plants where a high proportion of Se occurs as MeSeCys, *N. amplexicaulis* has on a different Se biopathway from this standard model, leading to SeCT accumulation (Nigam and McConnell, 1972; Burnell, 1981). Selenocystathionine formation is catalysed by the enzyme cystathionine-γ-synthase reacting with SeCys and O-phosphohomoserine (Dawson and Anderson, 1989). This enzyme, in both hyperaccumulators and non-accumulators, has a preference for Se over S compounds, which is important to note as SeCT formation is a rate limiting step to the formation of volatilised dimethyl selenide (DMSe) and essential to the effective metabolism of Se in dicot non-accumulators (Dawson and Anderson, 1989; Van Huysen et al., 2003; Drahoňovský et al., 2016). In non-accumulator species where cystathionine-γ-synthase was transgenically overexpressed, high rates of DMSe formation were observed, with lower or unchanged concentrations of within-tissue Se compounds (Van Huysen et al., 2003). Interestingly, *A. racemosus* was also reported to have both similar activity and Se preference in cystathionine-γ-synthase to *N. amplexicaulis*; most focus on this species shows that SeCys would normally be converted into MeSeCys, but SeCT has been reported in this species before (Martin et al., 1971; Dawson and Anderson, 1989; Sors et al., 2005).

4.3. Implications of the accumulation of selenocystathionine in *N. amplexicaulis*

The high fraction of SeCT suggests the pathway to SeMet and DMSe formation is possible, if not somehow bottlenecked. Smaller components of DMSeO in the tissues of old leaves (or stems and taproots) and potentially SeMet suggests DMSe-generating metabolism is still occurring. However, there is comparatively low Se in these tissues (Harvey et al., 2020). As SeCT is remobilised from these older tissues, perhaps lingering Se compounds continue the DMSe pathway; SeMet may not be toxic in these quantities, with volatilization aiding the eventual extraction of Se from these organs. It should be noted that DMSeO recorded here is the within-tissue compound, not the compound released by the plant.

Regardless, excessive Se presence in plants is always likely to lead to a diverse combination of Se compounds. The hyperaccumulator *Cardamine enshiensis* has a rather diverse combination of Se forms – including SeCT and a high proportion of selenolanthionine (Ouerdane et al., 2020). Other compounds of significance include selenohomolanthionine, which is formed along the pathway from SeCT to SeMet (Both et al., 2018), and SeCys, though the authors of that study noted that more in depth analysis was required (Yuan et al., 2013). *Lecythis minor*, which concentrates Se in its protein rich seeds, but rarely in other tissues, synthesises a high variety of derivatives of SeCT, selenohomocysteine, γ-glutamyl-selenocysteine and both freeform and protein bound SeMet (Dernovics et al., 2007; Németh et al., 2013).

Most comparative non-accumulators contain Se compounds further along the SeCys to DMSe pathway, such as SeMet in many crop plants and *B. juncea*, or Se-methyl-SeMet in several non-accumulator *Astragalus* species, which are relatively less toxic compared to SeCys (Virupaksha and Shrift, 1965; de Souza et al., 2000; Pilon-Smits and Quinn, 2010). When comparing the relative importance of SeCT in hyperaccumulators and non-accumulators, a good example is *Stanleya*: *S. pinnata*, which has been recorded with high proportions of MeSeCys and low proportions of SeCT, as explained by higher levels of SMT present in this species, whereas relative non-accumulator *S. albescens* contained SeCT, SeCys and selenate under spiked conditions (Freeman et al., 2010). Freeman et al. (2010) suggested that the accumulation of mixed MeSeCys and SeCT (or primarily SeCT) in plants lowered Se tolerance when compared to species that accumulated just MeSeCys (given the concentration of Se in primarily MeSeCys accumulating species in the *Astragalus* genus, compared to the concentrations seen in *N. amplexicaulis*).

4.4. Identification of methylselenocysteine in Neptunia heliophila

While *N. heliophila* is considerably less tolerant to environmental and within-tissue Se compared to *N. amplexicaulis,* hydroponically grown *N. heliophila* is still capable of accumulating fairly high concentrations of Se, higher than typically encountered in the natural habitat (McCray and Hurwood, 1963; Harvey et al., 2024, 2025). Furthermore, it does not 'exclude' Se from aerial tissues, and has a similar patterns of Se distribution to *N. amplexicaulis* (Harvey et al., 2025). However, *N. heliophila* does experience significant toxicity (as judged from the lowered biomass) at higher supplied concentrations of Se (~50 μM Se). Therefore, biochemical mechanisms for tolerance of Se are also present in *N. heliophila,* but different from the production of SeCT in *N. amplexicaulis*.

In this study, MeSeCys was identified in water extracts from *N. heliophila* using LC-tandem MS (Suppl. Fig. 8). Important caveats regarding this finding are that inorganic species (*e.g.,* Se(IV) and Se(VI)) and other Se organo-species may be present in samples that could not be identified by the LC-tandem MS used methodology (*e.g.,* below detection limits, ionisation mode, or observable natural Se-isotopic abundance in mass spectra). MeSeCys is not a typical Se species found in 'non-accumulators' (Schiavon and Pilon-Smits, 2017a; Lima et al., 2018). MeSeCys may be a relatively high abundance species in conjunction with many other relatively low Se species. MeSeCys formation in *N. heliophila* would likely develop from the reactions of a SMT enzyme. SMT in non-accumulators is often elusive - quantifiable MeSeCys production in non-accumulator species *Arabidopsis* and *B. juncea* only occurred in transgenic varieties which were overexpressing SMT (LeDuc et al., 2004). SMT isolated from a non-accumulator *Astragalus* species was an isoform incapable of synthesising MeSeCys (Sors et al., 2009). However, some Se tolerant species or secondary accumulators are capable of naturally synthesising MeSeCys, such as *Brassica oleracea*, from which SMT has been isolated previously (Lyi et al., 2005). *Neptunia heliophila* may similarly synthesise MeSeCys in the presence of elevated environmental Se, in concert with many other Se species, but without strong enough SMT activity to afford hyperaccumulator tolerance towards Se.

4.5. Inorganic forms of selenium

The presence of inorganic Se in plant organs can occur as the conversion of selenate to selenite is a rate limiting step towards SeCys formation (Zayed et al., 1998). Selenate was present in the stems and taproots of *N. amplexicaulis*; the stems of this plant show Se distribution throughout the pith and cortex (Figs. 1–4), areas where large volumes of selenate would not necessarily interfere or cause serious oxidative stress (Van Hoewyk, 2013). High proportions of selenate in the stipels of *N. amplexicaulis*, as seen in the XANES map, would achieve the same effect. Comparatively, minor amounts of selenate (such as in the leaves or fine roots) could also be attributed to rate limiting steps during the metabolism of Se, such as the reduction of selenate to selenite, or the reduction of selenite to selenide (Freeman et al., 2010; Lima et al., 2018). Bulk XAS analysis suggested that selenate-spiked plants contained lower proportions of selenate within organs compared to selenite dosed plants, whereas spatial XANES revealed the opposite pattern (Tables 3 and 4). There may be several factors effecting this discrepancy – uptake of selenate in hyperaccumulators is more efficient than the uptake of selenite, and uptake of Se in hydroponics is more efficient than in soil (Pilon-Smits et al., 1999; Harvey et al. unpublished). The rapid accumulation of selenate in hydroponics may be metabolically overwhelming, accounting for a buildup of selenate in plant organs. The accumulation from selenate dosed soil (or selenite dosed hydroponics) may just be slow enough to metabolise selenate efficiently with a strong expression of selenate reduction enzymes triggered by high Se uptake (Pilon-Smits et al., 1999). Selenite-dosed soils may have a much slower Se accumulation rate, which may not need to be metabolised as quickly. However, selenite may have oxidised to selenate in the soil prior to

uptake (Paydary et al., 2021). This may also account for lower uptake of Se in selenite dosed plants, considering lowered bioavailability of selenite under these conditions and time-staggered redox transformation into selenate (Hopper and Parker, 1999; Terry et al., 2000). Finally, while the presence of elemental Se on or in the roots is likely due to bacterial reduction, elemental Se as identified though spatial XANES may be metabolised from SeCys that is not directly metabolised into SeCT (Li et al., 2014; Van Hoewyk et al., 2005).

5. Conclusions

Selenocystathionine was found in *N. amplexicaulis,* while MeSeCys was found in *N. heliophila.* Understanding the molecular mechanisms behind SeCT synthesis will be the next step to better comprehend the importance of this compound. Extractable SeCT with a predictable Se content may be useful over a wide range of pharmaceutical and agricultural biofortication applications.

Author contributions

M-A.H., H.H.H., P.D.E. and A.V.D.E. conceptualized and designed the study. M-A.H grew and analysed chemical concentrations of the plant samples. M-A.H conducted the image distribution analysis. H.H.H., M-A.H., A.V.D.E., and P.D.E conducted the XAS experiment. H.H.H., J.I.V., C.J.K. and J.H.L. performed the XAS data analysis and interpretation. J.K.K. conducted the IC-MS and LC-MS and analysed and interpreted the data. M-A.H., A.V.D.E. H.H.H., J.K.K. and P.D.E wrote the manuscript.

Funding

This publication is part of the project "Living on the edge: unravelling the secrets of selenium hyperaccumulator plants" (with project number VI.Vidi.213.037) of the research programme ENW-VIDI which is (partly) financed by the Dutch Research Council (NWO). M-A. Harvey was the recipient of an Australian Government Research Training Program Scholarship.

Declaration of competing interest

The authors declare that they have no known competing financial interests or personal relationships that could have appeared to influence the work reported in this paper.

Acknowledgements

This research was undertaken using the X-ray Absorption (XAS) and X-ray Fluorescence Microscopy (XFM) beamlines at the Australian Synchrotron, part of ANSTO. We thank Bernt Johannessen (ANSTO) for support during the XAS experiment and Daryl Howard (ANSTO) during the XFM experiment and Jun Du (CSIRO) for help with the IC/LC-MS analysis.

Appendix A. Supplementary data

Supplementary data to this article can be found online at https://doi.org/10.1016/j.plaphy.2026.111091.

Data availability

Data used for this manuscript is available upon reasonable request to the corresponding author.

References

Anderson, J.W., 1993. Selenium interactions in sulfur metabolism. Sulfur nutrition and assimilation in higher plants: Regulatory, agricultural and environmental aspects. SPB Academic Publishing, The Hague, The Netherlands 49–60.
Beath, O.A., Gilbert, C.S., Eppson, H.F., 1939. The use of indicator plants in locating seleniferous areas in western United States. I. General. Am. J. Bot. 26 (4), 257–269.
Both, E.B., Shao, S., Xiang, J., Jókai, Z., Yin, H., Liu, Y., Magyar, A., Dernovics, M., 2018. Selenolanthionine is the major water-soluble selenium compound in the selenium tolerant plant *Cardamine violifolia*. Biochim. Biophys. Acta Gen. Subj. 1862 (11), 2354–2362.
Brown, T., Shrift, A., 1982. Selenium: toxicity and tolerance in higher plants. Biol. Rev. Camb. Phil. Soc. 57 (1), 59–84.
Burnell, J.N., 1981. Selenium metabolism in *Neptunia amplexicaulis*. Plant Physiol. 67 (2), 316–324.
Cao, M.-J., Wang, Z., Wirtz, M., Hell, R., Oliver, D.J., Xiang, C.-B., 2013. SULTR3;1 is a chloroplast-localized sulfate transporter in *Arabidopsis thaliana*. Plant J. 73 (4), 607–616.
Chen, Y.-C., Prabhu, K.S., Mastro, A.M., 2013. Is selenium a potential treatment for cancer metastasis? Nutrients 5 (4), 1149–1168.
Dawson, J.C., Anderson, J.W., 1989. Comparative enzymology of cystathionine and selenocystathionine synthesis of selenium-accumulator and non-accumulator plants. Phytochemistry 28 (1), 51–55.
de Souza, M.P., Lytle, C.M., Mulholland, M.M., Otte, M.L., Terry, N., 2000. Selenium assimilation and volatilization from Dimethylselenoniopropionate by Indian Mustard. Plant Physiol. 122 (4), 1281–1288.
Dernovics, M., García-Barrera, T., Bierla, K., Preud'Homme, H., Lobinski, R., 2007. Standardless identification of selenocystathionine and its γ-glutamyl derivatives in monkeypot nuts by 3D liquid chromatography with ICP-MS detection followed by nanoHPLC–Q-TOF-MS/MS. Analyst 132 (5), 439–449.
Dhillon, K.S., Bañuelos, G.S., 2017. Overview and prospects of selenium phytoremediation approaches. Selenium in Plants. Springer, pp. 277–321.
Drahoňovský, J., Száková, J., Mestek, O., Tremlová, J., Kaňa, A., Najmanová, J., Tlustoš, P., 2016. Selenium uptake, transformation and inter-element interactions by selected wildlife plant species after foliar selenate application. Environ. Exp. Bot. 125, 12–19.
Fordyce, F.M., 2013. Selenium deficiency and toxicity in the environment. Essentials of Medical Geology. Springer, pp. 375–416.
Freeman, J., Tamaoki, M., Stushnoff, C., Quinn, C.F., Cappa, J.J., Devonshire, J., Fakra, S., Marcus, M., McGrath, S.P., Van Hoewyk, D., et al., 2010. Molecular mechanisms of selenium tolerance and hyperaccumulation in *Stanleya pinnata*. Plant Physiol. 153 (4), 1630–1652.
Freeman, J.L., Zhang, L.H., Marcus, M.A., Fakra, S., McGrath, S.P., Pilon-Smits, E.A.H., 2006. Spatial imaging, speciation, and quantification of selenium in the hyperaccumulator plants *Astragalus bisulcatus* and *Stanleya pinnata*. Plant Physiol. 142 (1), 124.
Hartikainen, H., 2005. Biogeochemistry of selenium and its impact on food chain quality and human health. J. Trace Elem. Med. Biol. 18 (4), 309–318.
Harvey, M.-A., Erskine, P.D., Harris, H.H., Brown, G.K., Pilon-Smits, E.A.H., Casey, L.W., Echevarria, G., Van Der Ent, A., 2020. Distribution and chemical form of selenium in *Neptunia amplexicaulis* from Central Queensland, Australia. Metallomics 12 (4), 514–527.
Harvey, M.-A., Erskine, P.D., Harris, H.H., Virtue, J.I., van der Ent, A., 2024. Plant-soil relations of selenium, molybdenum and vanadium in the Richmond District of Central Queensland, Australia. Plant Soil 504, 435–455. https://doi.org/10.1007/s11104-024-06633-7.
Harvey, M.-A., Erskine, P.D., Harris, H.H., Pinto-Irish, K., Howard, D.L., Fabillo, M., van der Ent, A., 2025. Synchrotron X-ray fluorescence microscopy unveils selenium distribution and a phloem-sink hypothesis in *Neptunia amplexicaulis*. Plant Physiol. 199 (2). https://doi.org/10.1093/plphys/kiaf367 kiaf367.
Hopper, J.L., Parker, D.R., 1999. Plant availability of selenite and selenate as influenced by the competing ions phosphate and sulfate. Plant Soil 210 (2), 199–207.
Jones, M.W.M., Kopittke, P.M., Casey, L., Reinhardt, J., Blamey, F.P.C., van der Ent, A., 2019. Assessing radiation dose limits for X-ray fluorescence microscopy analysis of plant specimens. Ann. Bot. 125 (4), 599–610.
Kirkham, R., Dunn, P.A., Kuczewski, A.J., Siddons, D.P., Dodanwela, R., Moorhead, G.F., Ryan, C.G., De Geronimo, G., Beuttenmuller, R., Pinelli, D., et al., 2010. The Maia spectroscopy detector system: engineering for integrated pulse capture, low-latency scanning and real-time processing. AIP Conf. Proc. 1234 (1), 240–243.
Knott, S.G., McCray, C.W.R., 1959. Two naturally occurring outbreaks of selenosis in Queensland. Aust. Vet. J. 35 (7), 332–334.
LeDuc, D.L., Tarun, A.S., Montes-Bayon, M., Meija, J., Malit, M.F., Wu, C.P., AbdelSamie, M., Chiang, C.-Y., Tagmount, A., deSouza, M., et al., 2004. Overexpression of selenocysteine methyltransferase in Arabidopsis and Indian mustard increases selenium tolerance and accumulation. Plant Physiol. 135 (1), 377–383.
Lerotic, M., Mak, R., Wirick, S., Meirer, F., Jacobsen, C., 2014. MANTiS: a program for the analysis of X-ray spectromicroscopy data. J. Synchrotron Rad. 21, 1206–1212.
Leustek, T., Saito, K., 1999. Sulfate transport and assimilation in plants. Plant Physiol. 120 (3), 637–644.

Li, B., Liu, N., Li, Y., Jing, W., Fan, J., Li, D., Zhang, L., Zhang, X., Zhang, Z., Wang, L., 2014. Reduction of selenite to red elemental selenium by *Rhodopseudomonas palustris* strain N. PLoS One 9 (4), e95955.

Lima, L.W., Pilon-Smits, E.A.H., Schiavon, M., 2018. Mechanisms of selenium hyperaccumulation in plants: a survey of molecular, biochemical and ecological cues. Biochimica et Biophysica Acta General Subjects 1862 (11), 2343–2353.

Lobanov, A.V., Fomenko, D.E., Zhang, Y., Sengupta, A., Hatfield, D.L., Gladyshev, V.N., 2007. Evolutionary dynamics of eukaryotic selenoproteomes: large selenoproteomes may associate with aquatic life and small with terrestrial life. Genome Biol. 8 (9). R198-R198.

Lombi, E., Jonge, M., Donner, E., Ryan, C., Paterson, D., 2011. Trends in hard X-ray fluorescence mapping: environmental applications in the age of fast detectors. Anal. Bioanal. Chem. 400 (6), 1637–1644.

Lyi, S.M., Heller, L.I., Rutzke, M., Welch, R.M., Kochian, L.V., Li, L., 2005. Molecular and biochemical characterization of the selenocysteine Se-methyltransferase gene and Se-methylselenocysteine synthesis in broccoli. Plant Physiol. 138 (1), 409–420.

Martin, J.L., Shrift, A., Gerlach, M.L., 1971. Use of 75Se-selenite for the study of selenium metabolism in *Astragalus*. Phytochemistry 10 (5), 945–952.

McCray, C.W.R., Hurwood, I.S., 1963. Selenosis in north west Queensland associated with marine cretaceous formation. Queensland Journal of Agricutural Science (20), 475–498.

Mikkelsen, R.L., Page, A.L., Bingham, F.T., 1989. Factors affecting selenium accumulation by agricultural crops. In: Jacobs, L.W. (Ed.), *Selenium in Agriculture and the Environment* Madison, WI: Soil Science Society USA, pp. 65–94.

Montes-Bayón, M., LeDuc, D.L., Terry, N., Caruso, J.A., 2002. Selenium speciation in wild-type and genetically modified Se accumulating plants with HPLC separation and ICP-MS/ES-MS detection. Journal of Analytical Atomic Spectrometry 17 (8), 872–879.

Németh, A., García Reyes, J.F., Kosáry, J., Dernovics, M., 2013. The relationship of selenium tolerance and speciation in Lecythidaceae species. Metallomics 5 (12), 1663–1673.

Neuhierl, B., Böck, A., 1996. On the mechanism of selenium tolerance in selenium-accumulating plants. Eur. J. Biochem. 239 (1), 235–238.

Ng, B.H., Anderson, J.W., 1978. Synthesis of selenocysteine by cysteine synthases from selenium accumulator and non-accumulator plants. Phytochemistry 17 (12), 2069–2074.

Nigam, S.N., McConnell, W.B., 1972. Isolation and identification of l-cystathionine and l-selenocystathionine from the foliage of *Astragalus pectinatus*. Phytochemistry 11 (1), 377–380.

Ouerdane, L., Both, E.B., Xiang, J., Yin, H., Kang, Y., Shao, S., Kiszelák, K., Jókai, Z., Dernovics, M., 2020. Water soluble selenometabolome of *Cardamine violifolia*. Metallomics 12 (12), 2032–2048.

Papp, L.V., Lu, J., Holmgren, A., Khanna, K.K., 2007. From selenium to selenoproteins: synthesis, identity, and their role in human health. Antioxidants &Amp 9 (7), 775–806.

Paterson, D., De, Jonge M., Howard, D., Lewis, W., McKinlay, J., Starritt, A., Kusel, M., Ryan, C., Kirkham, R., Moorhead, G., 2011. The X-ray fluorescence microscopy beamline at the Australian synchrotron. AIP Conf. Proc. 219–222. American Institute of Physics.

Paydary, P., Schellenger, A.E.P., Teli, M., Jaisi, D.P., Onnis-Hayden, A., Larese-Casanova, P., 2021. Chemical oxidation of selenite to selenate: evaluation of reactive oxygen species and O transfer pathways. Chem. Geol. 575, 120229.

Peterson, P.J., Butler, G.W., 1961. The Uptake and Assimilation of Selenite by Higher Plants, pp. 126–146.

Peterson, P.J., Butler, G.W., 1967. Significance of selenocystathionine in an Australian selenium-accumulating plant, *Neptunia amplexicaulis*. Nature 213 (5076), 599–600.

Peterson, P.J., Robinson, P.J., 1972. L-cystathionine and its selenium analogue in *Neptunia amplexicaulis*. Phytochemistry 11 (5), 1837–1839.

Pickering, I.J., Wright, C., Bubner, B., Ellis, D., Persans, M.W., Yu, E.Y., George, G.N., Prince, R.C., Salt, D.E., 2003. Chemical form and distribution of selenium and sulfur in the selenium hyperaccumulator *Astragalus bisulcatus*. Plant Physiol. 131, 1460–1467.

Pilon-Smits, E.A., Quinn, C.F., 2010. Selenium metabolism in plants. Cell Biology of Metals and Nutrients. Springer, pp. 225–241.

Pilon-Smits, E.A., Quinn, C.F., Tapken, W., Malagoli, M., Schiavon, M., 2009. Physiological functions of beneficial elements. Curr. Opin. Plant Biol. 12 (3), 267–274.

Pilon-Smits, E.A.H., Garifullina, G.F., Abdel-Ghany, S., Kato, S.-I., Mihara, H., Hale, K.L., Burkhead, J.L., Esaki, N., Kurihara, T., Pilon, M., 2002. Characterization of a NifS-like chloroplast protein from *Arabidopsis*. Implications for its role in sulfur and selenium metabolism. Plant Physiol. 130 (3), 1309–1318.

Pilon-Smits, E.A.H., Hwang, S., Lytle, C.M., Zhu, Y., Tai, J.C., Bravo, R.C., Chen, Y., Leustek, T., Terry, N., 1999. Overexpression of ATP sulfurylase in Indian mustard leads to increased selenate uptake, reduction and tolerance. Plant Physiol. 119, 23–132.

Pilon-Smits, E.A.H., LeDuc, D.L., 2009. Phytoremediation of selenium using transgenic plants. Curr. Opin. Biotechnol. 20 (2), 207–212.

Pinto Irish, K., Harvey, M-A., Erskine, P.D., van der Ent, A., 2021. Root foraging and selenium uptake in the Australian hyperaccumulator *Neptunia amplexicaulis* and the non-accumulator *Neptunia gracilis*. Plant Soil 462 (1), 219–233. https://doi.org/10.1007/s11104-021-04843-x.

Pinto Irish, K., Harvey, M-A., Harris, H.H., Aarts, M.G.M., Chan, C.X., Erskine, P.D., van der Ent, A., 2023. Micro-analytical and molecular approaches for understanding the distribution, biochemistry, and molecular biology of selenium in (hyperaccumulator) plants. Planta 257, 2. https://doi.org/10.1007/s00425-022-04017-8.

Preud'homme, H., Far, J., Gil-Casal, S., Lobinski, R., 2012. Large-scale identification of selenium metabolites by online size-exclusion-reversed phase liquid chromatography with combined inductively coupled plasma (ICP-MS) and electrospray ionization linear trap-Orbitrap mass spectrometry (ESI-MS n). Metallomics 4 (5), 422–432.

Rayman, M.P., 2008. Food-chain selenium and human health: emphasis on intake. Br. J. Nutr. 100 (2), 254–268.

Rosenfeld, I., Beath, O.A., 1964. Selenium: Geobotany, Biochemistry, Toxicity and Nutrition. Academic Press, New York.

Rotruck, J.T., Pope, A.L., Ganther, H.E., Swanson, A.B., Hafeman, D.G., Hoekstra, W.G., 1973. Selenium: biochemical role as a component of glutathione peroxidase. Science 179 (4073), 588.

Ryan, C.G., 2000. Quantitative trace element imaging using PIXE and the nuclear microprobe. Int. J. Imag. Syst. Technol. 11, 219–230.

Ryan, C.G., Cousens, D.R., Sie, S.H., Griffin, W.L., 1990. Quantitative analysis of PIXE spectra in geoscience applications. Nucl. Instrum. Methods Phys. Res. Sect. B Beam Interact. Mater. Atoms 49, 271–276.

Ryan, C.G., Jamieson, D.N., 1993. Dynamic analysis: on-line quantitative PIXE microanalysis and its use in overlap-resolved elemental mapping. Nucl. Instrum. Methods Phys. Res. Sect. B Beam Interact. Mater. Atoms 77, 203–214.

Ryan, C.G., Kirkham, R., de Jonge, M.D., Siddons, D.P., van der Ent, A., Pagés, A., Boesenberg, U., Kuczewski, A.J., Dunn, P., Jensen, M., et al., 2018. The Maia Detector and event mode. Synchrotron Radiat. News 31 (6), 21–27.

Ryan, C.G., Kirkham, R., Hough, R.M., Moorhead, G., Siddons, D.P., de Jonge, M.D., Paterson, D.J., De Geronimo, G., Howard, D.L., Cleverley, J.S., 2010. Elemental X-ray imaging using the Maia detector array: the benefits and challenges of large solid-angle. Nucl. Instrum. Methods Phys. Res. Sect. A Accel. Spectrom. Detect. Assoc. Equip. 619 (1), 37–43.

Schiavon, M., Pilon-Smits, E.A.H., 2017a. The fascinating facets of plant selenium accumulation – biochemistry, physiology, evolution and ecology. New Phytol. 213, 1582–1596.

Schiavon, M., Pilon-Smits, E.A.H., 2017b. Selenium biofortification and phytoremediation phytotechnologies: a review. J. Environ. Qual. 46 (1), 10–19.

Schneider, C.A., Rasband, W.S., Eliceiri, K.W., 2012. NIH Image to ImageJ: 25 years of image analysis. Nat. Methods 9 (7), 671–675.

Schrauzer, G.N., 2001. Nutritional selenium supplements: product types, quality, and safety. J. Am. Coll. Nutr. 20 (1), 1–4.

Schwarz, K., Foltz, C.M., 1957. Selenium as an integral part of factor 3 against dietary necrotic liver degeneration. J. Am. Chem. Soc. 79 (12), 3292–3293.

Shao, S., Mi, X., Ouerdane, L., Lobinski, R., García-Reyes, J.F., Molina-Díaz, A., Vass, A., Dernovics, M., 2014. Quantification of Se-methylselenocysteine and its γ-glutamyl derivative from naturally Se-enriched green bean (*Phaseolus vulgaris vulgaris*) after HPLC-ESI-TOF-MS and orbitrap MS n-based identification. Food Anal. Methods 7 (5), 1147–1157.

Shrift, A., Ulrich, J.M., 1969. Transport of selenate and selenite into *Astragalus* roots. Plant Physiol. 44 (6), 893–896.

Siddons, D., Kirkham, R., Ryan, C., De Geronimo, G., Dragone, A., Kuczewski, A., Li, Z., Carini, G., Pinelli, D., Beuttenmuller, R., 2014. Maia X-ray microprobe detector array system. Journal of Physics: Conference Series. IOP Publishing, 012001.

Sors, T.G., Ellis, D.R., Salt, D.E., 2005. Selenium uptake, translocation, assimilation and metabolic fate in plants. Photosynth. Res. 86 (3), 373–389.

Sors, T.G., Martin, C.P., Salt, D.E., 2009. Characterization of selenocysteine methyltransferases from *Astragalus* species with contrasting selenium accumulation capacity. Plant J. 59 (1), 110–122.

Stadtman, T.C., 1990. Selenium biochemistry. Annu. Rev. Biochem. 59, 111–127.

Tagmount, A., Berken, A., Terry, N., 2002. An essential role of S-adenosyl-L-methionine: L-methionine S-methyltransferase in selenium volatilization by plants. Methylation of selenomethionine to selenium-methyl-L-selenium-methionine, the precursor of volatile selenium. Plant Physiol. 130 (2), 847–856.

Terry, N., Zayed, A.M., de Souza, M.P., Tarun, A.S., 2000. Selenium in higher plants. Annu. Rev. Plant Physiol. Plant Mol. Biol. 51 (1), 401–432.

van der Ent, A., Przybyłowicz, W.J., Jonge, M.D., Harris, H.H., Ryan, C.G., Tylko, G., Paterson, D.J., Barnabas, A.D., Kopittke, P.M., Mesjasz-Przybyłowicz, J., 2018. X-ray elemental mapping techniques for elucidating the ecophysiology of hyperaccumulator plants. New Phytol. 218, 432–452.

Van Hoewyk, D., 2013. A tale of two toxicities: malformed selenoproteins and oxidative stress both contribute to selenium stress in plants. Ann. Bot. 112 (6), 965–972.

Van Hoewyk, D., Garifullina, G.F., Ackley, A.R., Abdel-Ghany, S.E., Marcus, M.A., Fakra, S., Ishiyama, K., Inoue, E., Pilon, M., Takahashi, H., Pilon-Smits, E.A.H., 2005. Overexpression of AtCpNifS enhances selenium tolerance and accumulation in arabidopsis. Plant Physiol. 139 (3), 1518–1528.

Van Hoewyk, D., Takahashi, H., Inoue, E., Hess, A., Tamaoki, M., Pilon-Smits, E.A.H., 2008. Transcriptome analyses give insights into selenium-stress responses and selenium tolerance mechanisms in *Arabidopsis*. Physiol Plant 132 (2), 236–253.

Van Huysen, T., Abdel-Ghany, S., Hale, K.L., Leduc, D., Terry, N., Pilon-Smits, E.A., 2003. Overexpression of cystathionine-γ-synthase enhances selenium volatilization in *Brassica juncea*. Planta 218 (1), 71–78.

Virupaksha, T.K., Shrift, A., 1965. Biochemical differences between selenium accumulator and non-accumulator *Astragalus* species. Biochim. Biophys. Acta Gen. Subj. 107 (1), 69–80.
Weekley, C.M., Aitken, J.B., Finney, L., Vogt, S., Witting, P.K., Harris, H.H., 2013. Selenium metabolism in cancer cells: the combined application of XAS and XFM techniques to the problem of selenium speciation in biological systems. Nutrients 5 (5), 1734.
Weekley, C.M., Aitken, J.B., Witting, P.K., Harris, H.H., 2014. XAS studies of Se speciation in selenite-fed rats. Metallomics 6 (12), 2193–2203.
Weekley, C.M., Harris, H.H., 2013. Which form is that? The importance of selenium speciation and metabolism in the prevention and treatment of disease. Chem. Soc. Rev. 42 (23), 8870–8894.
White, P.J., 2016. Selenium accumulation by plants. Ann. Bot. 117 (2), 217–235.
White, P.J., Bowen, H.C., Parmaguru, P., Fritz, M., Spracklen, W.P., Spiby, R.E., Meacham, M.C., Mead, A., Harriman, M., Trueman, L.J., et al., 2004. Interactions between selenium and sulphur nutrition in *Arabidopsis thaliana*. J. Exp. Bot. 55 (404), 1927–1937.
Yuan, L., Zhu, Y., Lin, Z.-Q., Banuelos, G., Li, W., Yin, X., 2013. A novel selenocystine-accumulating plant in selenium-mine drainage area in Enshi, China. PLoS One 8 (6), e65615.
Zayed, A., Lytle, C.M., Terry, N., 1998. Accumulation and volatilization of different chemical species of selenium by plants. Planta 206 (2), 284–292.
Zeng, H., Combs, G.F., 2008. Selenium as an anticancer nutrient: roles in cell proliferation and tumor cell invasion. J. Nutr. Biochem. 19 (1), 1–7.
Zhao, F.-J., McGrath, S.P., 2009. Biofortification and phytoremediation. Curr. Opin. Plant Biol. 12 (3), 373–380.